Title

Effects of T1p Characteristics of Load-Bearing Hip Cartilage on Bilateral Knee Patellar Cartilage Subregions: Subjects With None to Moderate Radiographic Hip Osteoarthritis.

Journal

Journal of Magnetic Resonance Imaging, 60(1)

Authors

Bhattacharjee, Rupsa
Thahakoya, Rafeek
Luitjens, Johanna
et al.

Publication Date

2024-07-01

DOI

10.1002/jmri.29009

HHS Public Access

Author manuscript

J Magn Reson Imaging. Author manuscript; available in PMC 2024 July 28.

Published in final edited form as:

J Magn Reson Imaging. 2024 July ; 60(1): 186–202. doi:10.1002/jmri.29009.

Effects of $T_{1\rho}$ Characteristics of Load-Bearing Hip Cartilage on Bilateral Knee Patellar Cartilage Subregions: Subjects With None to Moderate Radiographic Hip Osteoarthritis

Rupsa Bhattacharjee, PhD[1,*], **Rafeek Thahakoya, PhD**[1], **Johanna Luitjens, MD**[1,2], **Misung Han, PhD**[1], **Koren E. Roach, PhD**[1], **Fei Jiang, PhD**[3], **Richard B. Souza, PT, PhD**[1,4], **Valentina Pedoia, PhD**[1], **Sharmila Majumdar, PhD**[1]

[1]Department of Radiology and Biomedical Imaging, University of California San Francisco, San Francisco, California, USA

[2]Department of Radiology, University Hospital, LMU Munich, Munich, Germany

[3]Department of Epidemiology and Biostatistics, University of California San Francisco, San Francisco, California, USA

[4]Department of Physical Therapy and Rehabilitation Science, University of California San Francisco, San Francisco, California, USA

Abstract

Background: The polyarticular nature of Osteoarthritis (OA) tends to manifest in multi-joints. Associations between cartilage health in connected joints can help identify early degeneration and offer the potential for biomechanical intervention. Such associations between hip and knee cartilages remain understudied.

Purpose: To investigate $T_{1\rho}$ associations between hip-femoral and acetabular-cartilage subregions with Intra-limb and Inter-limb patellar cartilage; whole and deep-medial (DM), deep-lateral (DL), superficial-medial (SM), superficial-lateral (SL) subregions.

Study Type: Prospective.

Subjects: Twenty-eight subjects (age 55.1 ± 12.8 years, 15 females) with none-to-moderate hip-OA while no radiographic knee-OA.

Field Strength/Sequence: 3-T, bilateral hip, and knee: 3D-proton-density-fat-saturated (PDFS) Cube and Magnetization-Prepared-Angle-Modulated-Partitioned-k-Space-Spoiled-Gradient-Echo-Snapshots (MAPSS).

Assessment: Ages of subjects were categorized into Group-1 (≤40), Group-2 (41–50), Group-3 (51–60), Group-4 (61–70), Group-5 (71–80), and Group-6 (≥81). Hip $T_{1\rho}$ maps, co-registered

[*]Address reprint requests to: R.B., Center of Intelligent Imaging (CI), QB3 Building, Byers Hall, 2nd Floor, Suite BH-201, 1700 – 4th Street, San Francisco, CA, 94158, USA. rupsa.bhattacharjee1@gmail.com or rupsa.bhattacharjee@ucsf.edu.

Additional supporting information may be found in the online version of this article

to Cube, underwent an atlas-based algorithm to quantify femoral and acetabular subregional (R_2–R_7) cartilage $T_{1\rho}$. For knee Cube, a combination of V-Net architectures was used to segment the patellar cartilage and subregions (DM, DL, SM, SL). $T_{1\rho}$ values were computed from co-registered MAPSS.

Statistical Tests: For Intra-and-Inter-limb, 5 optimum predictors out of 13 (Hip subregional $T_{1\rho}$, age group, gender) were selected by univariate linear-regression, to predict outcome (patellar $T_{1\rho}$). The top five predictors were stepwise added to six linear mixed-effect (LME) models. In all LME models, we assume the data come from the same subject sharing the same random effect. The best-performing models (LME-$model_{best}$) selected via ANOVA, were tested with DM, SM, SL, and DL subregional-mean $T_{1\rho}$. LME assumptions were verified (normality of residuals, random-effects, and posterior-predictive-checks).

Results: LME-$model_{best}$ (Intra-limb) had significant negative and positive fixed-effects of femoral-R_5 and acetabular-R_2 $T_{1\rho}$, respectively (conditional-R^2 = 0.581). LME-$model_{best}$ (Inter-limb) had significant positive fixed-effects of femoral-R_3 $T_{1\rho}$ (conditional-R^2 = 0.26).

Data Conclusion: Significant positive and negative $T_{1\rho}$ associations were identified between load-bearing hip cartilage-subregions vs. ipsilateral and contralateral patellar cartilages respectively. The effects were localized on medial subregions of Inter-limb, in particular.

Evidence Level: 1

Technical Efficacy: Stage 1

Osteoarthritis (OA) is the most prevalent form of arthritis and is related to a serious health crisis.[1] It causes a tremendous amount of functional burden and social isolation with limiting work and activity levels in the lives of approximately 32.5 million US adults.[1] Prediction studies foresee approximately 11.4% of adults experiencing OA-attributable activity limitations by the year 2040,[2] and those are even worse for patients with concurrent conditions, such as sleep deprivation, anxiety, obesity, hypertension, and diabetes.[3] The overall economic expenditure is projected at 17 billion in indirect lost earnings and 65 billion annually in direct medical expenses,[4] with a greater percentage of patients ultimately opting for total joint-replacement.[3]

The polyarticular nature of OA studies[5] tends to manifest in more than one joint. Prierto-Alhambra et al.[6] have reported that knee OA can predict the occurrence of an eventual hip OA. On the other hand, 45% of lone hip OA patients have been shown to develop subsequent knee OA.[7] Patients undergoing hip-replacement and developing progressive knee OA in the following decade had been reported to have a higher chance of the contralateral knee being affected than the ipsilateral with a 2.4:1 ratio.[8] Age has been deduced as an important factor in developing single-joint OA.[6] However, there is a lack of consensus in reported literature, on higher probabilities of developing bilateral or multi-joint OA systemically alone as a factor of age or gender.[7] Such findings lead to the speculation of whether the propagation of OA is possibly favorable in joints that are anatomically closer or mechanistically connected, such as the hip and the knee, on which the reported literature is seemingly limited.[9]

The possibility of mechanistically connected joints being vulnerable to OA propagation remains even more crucial from a prevention point of view. A compartment-specific assessment of degrading or preserved knee cartilage in association with degrading, already impaired, or normal-appearing hip cartilage, can potentially help to understand the multi-joint connection if done in a timely manner. Having developed OA, joints have fewer chances of complete cure[10] with very limited treatment options. Targeted physical therapies,[11] pain and inflammation control drugs,[12] and lifestyle modifications have proven to help manage the conditions. However, prior knowledge of location-specific early-stage degradation of knee cartilage can be extremely helpful if the tissue is not yet fully lost, and initial extents of cartilage abnormalities can at least be arrested. Timely information on localized degenerative patterns might also be potentially utilized for identifying the right candidates for clinical trials for emerging pharmaceutical therapies[13] or targeted treatments. In fact, often improvements in hip strength and coordination are suggested as part of rehabilitation programs to manage patellofemoral pain and discomfort.[14]

With degrading hip cartilage, an individual can be observed to have altered gait patterns.[15] Balancing the bodily mechanical load in sync with existing hip disability or pain can lead to unusual loading of the contralateral knee joint while walking or performing daily activities. Previous work provides copious examples[14] of meaningful associations between overall hip weakness, hip abductor weakness specifically, and abnormal hip kinematics during various tasks in patients with patellofemoral pain,[16] which is often a precursor to developing patellofemoral joint (PFJ) OA. Peak knee flexion moment and knee flexion moment impulse during the second half of the stance are reported to be related to the progression of PFJ-OA.[17] Additionally, patellar malalignment is proven detrimental[18] to the patellofemoral cartilage and can be mediated by abnormal gait kinematics. However, there is a lack of reported literature on whether the negative effects of degenerative hip cartilage and associated gait imbalances might be propagated to the knees.[19]

Initial degradation of cartilage starts with loss of proteoglycan content, increase in water content, and disruption of the collagen network.[20] These changes over time can lead to broader extents of irreversible morphological cartilage damage and narrowing of joint spaces.[21] Quantitative MRI, specifically $T_{1\rho}$ and T_2 mapping[22] have been quite well established for generating compositional imaging biomarkers to depict such microscopic extents of early cartilage changes, even in an asymptomatic population.[23] Be it in the hip[20] or the knee, elevated $T_{1\rho}$ and T_2 time measurements can indicate early cartilage degeneration long before the cartilage is fully damaged beyond repair, and starts showing up in morphological MRI with abnormalities. Therefore, for the evaluation of early cartilage changes in the hip and knee, $T_{1\rho}$ and T_2 mapping remains one of the various quantitative tools of choice.

We hypothesized characterization of hip cartilage might be one of the deciding factors for how apparently normal patellofemoral cartilage would eventually degenerate over time. The Intra-limb and Inter-limb unidirectional propagation (from hip to knee cartilages) of varied extents of degenerative changes might be possible across a diverse cohort of subjects with none to moderate hip OA and with no pre-existing radiographic knee OA. Such early effects of associations might possibly be driven by proteoglycan changes and might thus

be quantified via $T_{1\rho}$ relaxation of cartilages. Therefore, the aims of this study were to 1) investigate the patterns of hip (femoral and acetabular) and knee patellar cartilage $T_{1\rho}$ associations via statistical modeling, and to 2) examine whether such Inter- or Intra-limb hip $T_{1\rho}$ associations might also be observed with the further smaller patellar sub-regions (deep, superficial, medial, and lateral).

Materials and Methods

In this ongoing prospective multi-joint study, approved by the local Institutional Review Board (IRB), subjects with hip OA and control subjects were recruited for simultaneous bilateral acquisitions. Written informed consent was provided by the subjects prior to data collection.

Subjects

The subjects were recruited from previously published hip study cohorts[20,24] as part of the hip clinical examination and care-plan services by the Orthopedic clinic on campus. Study inclusion was confirmed by prior bilateral hip anterior–posterior screening radiographs according to the standard-in-practice Kellgren–Lawrence (KL) scoring,[25] assessed by a musculoskeletal radiologist (JL, with 3 years of training). The prior radiographic KL-scoring was used to characterize the extent of disease severity as healthy (KL-score of 0), early-to-moderate hip OA (KL-score of 1 to 3) for both hips, and to identify subjects as the healthy controls or having hip OA. Exclusion in this study was defined as either of the hips having advanced stages of OA (KL-score = 4). In addition, the following set of inclusion criteria was considered: 1) being above 18 years of age, 2) having no previous history of surgery on either hip or knee, 3) absence of clinically diagnosed knee OA, 4) absence of a recent history of trauma in the past 3 months before recruitment, 5) absence of any intraarticular injection in the past 6 months of recruitment, 6) absence of sickle cell disease, hemoglobinopathy, inflammatory arthropathy, hematochromatosis, and contraindications to MRI. The subjects having fulfilled the required criteria underwent MRI acquisitions during the period of December 2021 to March 2023 for inclusion in this multi-joint study.

Age Groups

To avoid using age as a random continuous variable or as crudely grouped literary templates (young-adults, middle-ages, elders, etc.), the age value of each subject was categorized into six consistent clusters: ages being ≤40 as Group-1, 41–50 as Group-2, 51–60 as Group-3, 61–70 as Group-4, 71–80 as Group-5, and ≥81 as Group-6, respectively.[26]

MRI Acquisition

All participants underwent MRI scan acquisitions in a 3.0 T GE Signa Premier scanner (GE Healthcare, Waukesha, WI, USA) for simultaneous bilateral hip and simultaneous bilateral knee imaging. The subjects were positioned supine, feet-first as demonstrated in Fig. 1. A 30-channel adaptive-image-receive anterior array coil and a 60-channel spine posterior-array coil embedded into the table were combined for bilateral hip acquisitions.[27] Shim volumes were located on each hip for better uniform B0/B1 fields over the joints. Two 16-channel

medium flex receive-only coils (NeoCoil, Pewaukee, WI, USA) were wrapped around each knee for bilateral knee acquisitions.

Shims and center frequencies were automatically calculated based on left and right shim volumes, for ensuring uniform fat suppression on simultaneous bilateral knee acquisitions. Bilateral three-dimensional (3D) proton-density fat-saturated fast-spin-echo (3D PDFS FSE, i.e., Cube) and bilateral Magnetization-Prepared Angle-Modulated Partitioned k-Space Spoiled Gradient Echo Snapshots (MAPSS) sequences were acquired for both hips and knees for morphological and compositional (combined $T_{1\rho}$ and T_2) assessments, respectively. The detailed scanning protocol is summarized in Table 1.

Image Processing and Analysis

All analyses were performed using an in-house program developed in MATLAB (version R2021a, The MathWorks Inc., Natick, MA, USA) unless otherwise noted. The stepwise pipeline for image processing and analysis is demonstrated in Fig. 1. Following the methodology explained in the sections below, we evaluated both $T_{1\rho}$ and T_2 relaxation values for both hips and knees. However, in this study, we have investigated $T_{1\rho}$ associations alone for multi-joint connectivity.

Image Splitting Into Left and Right Stacks

Bilateral hip and knee, Cube, and MAPSS images were automatically divided into left and right image-stacks. From this point onwards, the left and right hip images of each subject were treated separately as two individual hips as well as knees.

Bilateral Hip and Knee: $T_{1\rho}$ Mapping

The algorithms for mapping multi-echo images into $T_{1\rho}$ relaxation times, for the hip[20] and knee[28] were developed independently, but similar in nature. Multi-echo images corresponding to multiple spinlock times (TSLs) and echo times (TEs) were rigidly co-registered to the first echo image shared between TE and TSL (TE = 0 msec, TSL = 0 msec). The $T_{1\rho}$ maps were obtained thereafter by fitting multiple TSLs and TEs corresponding to the images by Levenberg–Marquardt mono-exponential equation, on a per-voxel basis,[20] considering $S_{TSL} \propto e^{-\frac{TSL}{T1\rho}}$

Bilateral Hip $T_{1\rho}$ Quantification: Atlas-Based Approach

The fitted hip $T_{1\rho}$ maps underwent a previously validated atlas-based algorithmic approach.[23,24] The first-echo MAPSS images were first nonrigidly registered to a previously defined single-reference atlas[20] space having minimal average deformation. The registration transformation field was subsequently applied to the remaining echo-images as well as the fitted $T_{1\rho}$ maps. Manually segmented femoral and acetabular cartilage masks and further sub-segmentations[24] on the reference atlas were applied on $T_{1\rho}$ maps of every patient, to automatically isolate the subregions on four two-dimensional (2D) slices of the acetabular and femoral cartilage on each participant. The eight subregions (as demonstrated in Fig. 1, R_1–R_8) follow a general clock position terminology. These can broadly be classified as R_2 as posterior, R_3 as posterior-superior, R_4 as superior, R_5 as anterior-superior, R_6 as anterior, and

R_7 as anterior-inferior cartilage regions,[29] as marked in Fig. 1. Specifically, R_1 and R_8 are regions with no viable cartilage to assess. The analysis yielded $T_{1\rho}$ of femoral and acetabular subregional (R_2–R_7) cartilages.[23,24]

Bilateral Knee Patellofemoral $T_{1\rho}$ Quantification: Deep Learning-Based Approach

For knees, a deep learning (DL)-based cartilage segmentation approach was employed. Two 3D V-Net architectures validated previously[30] were applied consecutively on the stack of each single-knee Cube images with 512 × 512 reconstruction matrix size. The first one, a five-class model[30] segmented the Cube knee images into femoral, tibial, patellar cartilages, meniscus region, and background, respectively. The second model takes the first channel output as its input and further segments the five classes into 11[30]: medial, lateral femoral (MFC, LFC), medial, lateral tibial (MTC, LTC), trochlear (Tro), patellar cartilage, four menisci horns, and the background. The first-echo MAPSS images and $T_{1\rho}$ maps were geometrically resampled from their respective digital imaging and communications in medicine (Dicom)-based anatomical coordinate spaces to the voxel space and co-registered[31] with the voxel space constituting the Cube images. Finally, six cartilage masks (LFC, MFC, LTC, MTC, Tro, and Patellar) segmented from the Cube images were used for analysis. The $T_{1\rho}$ relaxation values for six sub-regional knee cartilages were automatically extracted by averaging the compartmental $T_{1\rho}$ maps for all slices. In the scope of this study, the focused attention was on the PFJ. Therefore, in addition to the whole cartilage mean $T_{1\rho}$, the patellar cartilages were further automatically subdivided based on anatomical positioning (medial/lateral) and cartilage depth (deep/superficial) into four subregions: deep-medial (DM), deep-lateral (DL), superficial-medial (SM), and superficial-lateral (SL).[32] Mean $T_{1\rho}$ values were computed for each of the four subregions of the patellar cartilage. An upper clipping threshold (100 msec for hips, 120 msec for knees) was applied while averaging the $T_{1\rho}$ on all the instances, to avoid stray pixels that might have been influenced by any nearby fluid presence, minuscule misregistration, or partial volume.

Statistical Analysis

All analyses have been performed using RStudio (version 12.0+353; https://www.r-project.org/), with the “rcompanion,” “lmtest,” “lme4,” and “flexplot” packages in particular.

PREDICTOR VARIABLES.—The age groups, gender, subregional mean $T_{1\rho}$ of hip femoral (R_2–R_7), and acetabular (R_2–R_6) cartilages were considered as predictor variables.

OUTCOMES.—Knee patellar $T_{1\rho}$ values (mean of whole cartilage) were considered as primary outcome variables. Mean $T_{1\rho}$ of knee patellar DM, SM, SL, and DL subregions were defined as secondary outcomes.

We studied the effects of predictors on the primary outcome and the secondary outcomes in the following two case scenarios.

1. Case 1: Intra-limb analysis: Primary and secondary outcomes are patellar cartilage $T_{1\rho}$ from the ipsilateral knee.

2. Case 2: Inter-limb analysis: Primary and secondary outcomes are patellar cartilage $T_{1\rho}$ from the contralateral knee.

A common analysis and reporting structure has been implemented in both cases, as demonstrated in Fig. S1 in the Supplemental Material, and explained briefly below in three major steps. Under all analysis circumstances, *P*-values were computed from Wald test based on asymptotic t-distributed test statistics.

In Step-1, 13 linear models (estimated using Ordinary-least-square regression) were individually fitted to predict the primary outcome with each of the 13 predictor variables with a relationship:

$$y = \beta_i x_i + b, \tag{1}$$

where, x_i represented the i th predictors, where $i = 1$ to 13, and y was the primary outcome (as per cases 1, 2, 3, or 4). A log-likelihood ratio test was performed to study whether adding the specific predictor subsequently reduced the regression error compared with the null model with no predictor. The top five individual predictors were identified for a subsequent linear mixed-effects model (LME) analysis based on the combination of lowest *P*-values, corrected Akaike-Information-Criterion (AICc), and Bayesian-Information-Criterion (BIC) values as shown in Tables S1 and S2 in the Supplemental Material.

In Step-2, for each case, given the top five predictors, the best LME model was identified using a forward stepwise method as explained in Appendix-I and illustrated in Fig. S1 in the Supplemental Material. The final model (Model-6) was an LME model with five predictors and γ as a random effect that accounted for the correlation among the samples from the same subject, considering bilateral data. The within-subject correlation is assumed to have an "exchangeable" structure during the estimation. All the models were estimated using maximum-likelihood and nloptwrap optimizer. The statistical significance of the six models was compared via one-way analysis of variance (ANOVA). The statistically significant model with the best predictive ability was identified based on comparing the models' explanatory power, i.e., goodness of fit statistics (via marginal and conditional R^2 values). Whether adding a predictor as a fixed-effect term to the best model significantly affected the primary outcome was assessed via the *P*-value and Intra-class-coefficient (ICC). The assumptions, i.e., normality of residuals, normality of random-effects, and posterior predictive checks were assessed for the best-performing model for both cases ($\text{best-model}_{\text{case1}}$ and $\text{best-model}_{\text{case2}}$).

In Step-3, the best-performing model ($\text{best-model}_{\text{case1}}$ and $\text{best-model}_{\text{case2}}$) with one or more predictors was then further analyzed for associations with secondary outcomes of ipsilateral or contralateral knee as per cases 1 or 2, respectively.

$$y_j = \beta_{0j} + \beta_{1j}^{\top} x_{best\,j} + \gamma_j + \varepsilon, \tag{2}$$

where y_1 = DM, y_2 = DL, y_3 = SM, and y_4 = SL subregional mean cartilage $T_{1\rho}$, and $x_{best\,j}$ was a vector of predictors for the jth outcome in the best-performing model, as chosen from Step-2. Goodness-of-fit, P-values, ICC, and model assumptions were assessed as mentioned earlier, in Step-2.

For all statistical testing, the significance threshold was set at alpha level $P \leq 0.05$

Results

Participant Characteristics

A total of 31 subjects were initially recruited. Twenty-eight subjects with 56 hips and knees (15 females and 13 males, age: 55.1 12.8 years, Body-Mass-Index [BMI]: 24.08 3.66 kg/m) fulfilled all criteria and were recruited in this study. Based on radiographic assessment, 46 hips were categorized as healthy controls, and 10 hips were categorized as having mild-to-moderate hip OA. The demographic details along with KL-scores, and mean $T_{1\rho}$ for hip (femoral R_2–R_7, acetabular R_2–R_6) and knee patellar cartilage (whole, DM, DL, SM, and SL) subregions are summarized in Table 2.

Case 1: Intra-Limb Analysis

Step-1: The top predictor variables observed in the univariate linear regression analysis (summarized in Table S1 in the Supplemental Material) were mean $T_{1\rho}$ for hip femoral R_5, R_6, R_7, acetabular R_2 subregions, and gender.

Step-2: Performances of the six LME models, fitted by adding these five predictors stepwise, are summarized in Table 3. The best predictor model observed was Model-3, being statistically significant, with the highest ICC, marginal and conditional R^2, implying the best fit considering Participant-ID as random-effect. The best predictor model (Model-3) for ipsilateral knee patellar $T_{1\rho}$ (mean of whole cartilage) had fixed effect contributions from two predictors: mean $T_{1\rho}$ of hip femoral R_5 cartilage (negative, estimate = −0.56, standardized-effect = −0.737, 95% CI = −0.84 to −0.27) and acetabular R_2 cartilage (positive, estimate = 0.71, standardized-effect = 0.757, 95% CI = 0.36 to 1.06). The model's total explanatory power was substantial (conditional R^2 = 0.581), and the part related to the fixed-effects alone (marginal R^2) was 0.352. The model's intercept (corresponding to fixed-effec ts = 0) was 44.70 (95% CI [30.61 to 58.79]).

Step-3: Performances of the best LME model (Model-3, selected from Step-2), evaluated for finding associations with secondary outcomes, ipsilateral limb knee patellar (subregional cartilages, DM, SM, SL, and DL) mean $T_{1\rho}$, are summarized in Table 4. For all subregions (DM, SM, SL, and DL), the model's explanatory power was moderate to substantial (conditional R^2 = 0.273, 0.394, 0.191, 0.232, respectively). The mean $T_{1\rho}$ value of hip acetabular R_2 cartilage and hip femoral R_5 cartilage were found to be significant positive and negative predictors respectively associated with all subregions.

Case 2: Inter-Limb Analysis

Step-1: The top predictor variables observed in the univariate linear regression analysis (summarized in Table S2 in the Supplemental Material) were mean $T_{1\rho}$ of hip femoral cartilage R_7, age group, gender, mean $T_{1\rho}$ of femoral cartilage R_6, and femoral cartilage R_3.

Step-2: Performances of the six LME models, fitted by adding these five predictors stepwise, are summarized in Table 5. The best predictor model observed was Model-6, statistically significant, with the highest ICC, marginal and conditional R^2, implying the best fit considering Participant-ID as random-effect. The best predictor model (Model-6) for contralateral knee patellar $T_{1\rho}$ (mean of whole cartilage) had significant fixed effect contributions from: mean $T_{1\rho}$ of hip femoral R_3 (positive, estimate = 0.59, standardized-effect = 0.375, 95% CI = 0.01 to 1.18). The model's total explanatory power was moderate (conditional R^2 = 0.26), and the part related to the fixed-effects alone (marginal R^2) was 0.19. The model's intercept (corresponding to fixed-effects = 0) was 39.53 (95% CI [21.32 to 57.74]). Table 5 shows that the effects of other four predictors in this model (mean $T_{1\rho}$ of hip femoral R_6 cartilage, femoral R_7 cartilage, age group, and gender); however additive, were statistically non-significant (P = 0.675, 0.074, 0.791, 0.072, respectively).

Step-3: Performance of the best LME model (Model-6, selected from Step-2), as evaluated for finding associations with secondary outcomes, contralateral limb knee patellar (subregional cartilages, DM, SM, SL, and DL) mean $T_{1\rho}$, are summarized in Table 6. Mean $T_{1\rho}$ of hip femoral R_3 and R_7 cartilages were found to be significant positive and negative predictors, respectively, associated with SM subregions. Age group was found to be a significant positive predictor associated with DM and SM subregions. No predictors of the model were found to be significantly associated with the lateral subregions (DL and SL).

Intra and Inter-limb analysis results are summarized into demonstrative examples (Fig. 2) and pictorial representations (Figs. 3 and 4).

Discussion

This study investigated $T_{1\rho}$ association patterns between hip cartilage subregions with knee patellar cartilages, both Intra-limb, and Inter-limb, in a cohort consisting of a mix of normal as well as subjects with radiographic hip OA. LME modeling equations were identified to characterize Intra-limb and Inter-limb knee patellar cartilage $T_{1\rho}$, at the current time point, from compositional profiling of hip femoral and acetabular cartilage subregion $T_{1\rho}$. Posterior-superior (acetabular R_2) and posterior (femoral R_3) cartilage subregional $T_{1\rho}$ were observed to show significant positive effects, in the predictive mean $T_{1\rho}$ profiling of the ipsilateral and contralateral knee patellar whole cartilage. On the contrary, anterior (femoral R_5) hip cartilage subregional $T_{1\rho}$ negatively affected just the ipsilateral knee patellar whole cartilage mean $T_{1\rho}$. These findings suggest that degeneration of the posterior regions of the hip joint is associated with concurrent degeneration of both same-side and opposite-side patellar cartilages. However, degeneration of the anterior region of the hip joint was associated with preservation of the patellar cartilage on the same limb.

The current study explored distinctions between hip vs. Intra-limb or Inter-limb patellofemoral cartilage compositional associations, with bilateral hip and knee compositional and morphological data, providing results for examining joint degeneration across multiple joints. Additionally, the LME models were designed carefully to avoid confounding factors generated by random between-subject effects. The primary hypothesis of the study relied on individuals with a varied range of compositional hip cartilages likely demonstrating altered gait patterns depending on degenerative severity, thereby affecting both the Intra- and Inter-limb PFJs. The multifold associations revealed in this study can thus be predictive of the extent to which the changes in specific hip cartilage subregion $T_{1\rho}$, positively or negatively, affect the patellar cartilage. A stringent inclusion criterion of no prior incidence of radiographic knee OA in either of the knees is enforced in this mixed-cohort generalized association study. This suggests that the observed hip and knee subregional associations can either be mechanistic or systemic, but most definitely not influenced by an additional presence of knee OA or already altered patellar subregional $T_{1\rho}$.

Degenerative changes caused by long-term load-bearing stress[33] in the hip cartilage have long been reported to have nonuniform regional variations.[29] These regional degenerations tend to be spatially localized on the high-load-bearing areas,[34,35] such as the posterior-superior, superior, and anterior-superior regions (R_2, R_3, R_4, R_5) of both the femoral and acetabular cartilages. Even healthy controls have been reported to demonstrate a certain extent of topographic variations in T_2,[36] caused by load-bearing distributions across these cartilage subregions. The femoral R_3 subregional $T_{1\rho}$ has previously been documented to be a significant predictor in a larger cohort of hip OA progression study.[20] Although this current study did not focus on subregional hip cartilage $T_{1\rho}$ variations, our region-specific automatized atlas-based approach seems to be beneficial in identifying sensitive load-bearing regions with variational $T_{1\rho}$, having significant positive or negative effects on the Intra-limb or Inter-limb patellar cartilage, while other regions do not.

The theoretical understanding of weight-bearing hip cartilages experiencing $T_{1\rho}$ variations, and thereby propagating those variations to affect the intra and Inter-limb patellar cartilage, may justify the compositional associations. A subject experiencing a prolonged $T_{1\rho}$ in the load-bearing femoral R_3 or R_5 subregions most likely tends to balance the pain and discomfort via load-balancing and thereby altering the gait pattern to exert a higher load on the weight-bearing contralateral patellar cartilage and providing a compensatory relief to the ipsilateral patellar cartilage or vice-versa. This hypothetical mechanism can explain the positive (femoral R_3 vs contralateral patellar) and negative associations (femoral R_5 vs ipsilateral patellar) observed for Inter-limb and Intra-limb assessments, respectively. The ipsilateral hip-knee load-bearing relationship is definitely multi-directional. Another possibility of a similar but opposite ongoing gait-altering and load-balancing mechanism was observed, which positively connects the prolongation or decrease of acetabular R_2 and ipsilateral patellar-cartilage $T_{1\rho}$. Adding to it, subregions of the hip cartilage significantly affecting the Intra-limb knee (positively or negatively; acetabular R_2 and femoral R_5, respectively), weight-bearing or not, are not necessarily the exact same subregions affecting the Inter-limb situation (positively; femoral R_3). Therefore, the underlying mechanisms behind the hip-cartilage subregional $T_{1\rho}$ vs. the ipsilateral or contralateral patellar cartilage $T_{1\rho}$ associations can be diverse as well.

Similarly, not all smaller subregions of the patellar cartilage bear positive or negative associations with the hip cartilage, with the same effect. Further analysis of the knee domain revealed that the significant positive associations of the hip load-bearing $T_{1\rho}$ predictors were all localized only on the medial subregions of the contralateral patellar cartilage (DM and SM), with no involvement noted on the lateral sub-regions (DL and SL). However, for the ipsilateral knee, all subregions (DM, SM, DL, and SL) of the patellar cartilage significantly bored the positive and negative effects of the load-bearing hip $T_{1\rho}$ predictors. Superficial regions have been historically often more sensitive to smaller changes, especially damages,[37] compared to the deeper layers. Previous work showed[38] alignment and geometry measures, such as patella alta, patellar tilt, medial translation, or trochlear geometry were often associated with cartilage abnormalities as well as higher and altered $T_{1\rho}$ times in the PFJ. Therefore, from a mechanistic point of view, it is not hard to imagine the gait patterns or kinematics of an individual would differ sufficiently between medial and lateral cartilage regions, thereby associating a positive or negative effect from the hip cartilage in either of the medial or lateral while none on the other.

Population-based research on OA has identified higher-age females to be at the most risk of high incidence, with a peak of risk around menopause.[6] Hip OA, on the contrary, is somewhat less common in aging cohorts than other joint OA.[39] Our study attempted predictive profiling of patellar $T_{1\rho}$, in which the age group is observed as a significant predictor in Inter-joint analysis of medial subregions, but not of the whole patellar cartilage or lateral subregions. In this cohort, subjects in higher age groups experienced increased patellar $T_{1\rho}$, more so medially. The active biological age-related matrix degradation and oxidative stress[39] might be prevalent on the medial layers of patellar cartilage as compared to lateral. Nevertheless, the possibility of altering gait patterns and alignments due to age-related movement discomforts, balancing the majority of the load on the medial side of the contralateral patella, cannot be ruled out. Combining mediation analyses with kinetic parameters might help explain the sequence of biological and mechanical effects, simultaneous or chronological.

In addition to age, mean $T_{1\rho}$ of femoral R_6, R_7 cartilage, and gender had additive fixed-effects on the Inter-limb outcome, albeit, non-significant. These two anterior regions might have gender-driven involvement and differences in counterbalancing the load. That will affect the kinetic patterns of an individual thereby affecting the contralateral medial patellar cartilage heterogeneously. Such specific mechanisms might also be prominent in a gender-stratified analysis of a larger cohort. The observed data in this study is insufficient to make conclusions to that end.

This leads us to speculate all possible root causes of such multi-joint connections as the ones observed in this study. The varied connections and associations, although established, might not all be caused directly or mediated by altered gait patterns and mechanistic translations of asymmetric loading. There could also be a smaller subset of systemic changes and associations in the bigger multi-joint connectivity picture between the hip and Intra- or Inter-limb knee. If the associations are directly caused by altered gait patterns and compensatory movement mechanisms, then these would also be apparently mediated by ground reaction forces, rate of loading, or knee and hip flexion and extension moments. On the contrary, if

the associations are systemically propagated and reflective of the generalized multi-joint OA phenotype,[8] the mediation effects might not be a prerequisite. The direct flow of causality between variations in hip subregional $T_{1\rho}$, altered gait, asymmetric loading, and patellar subregional $T_{1\rho}$ variations remains unclear in all of these associations observed in our study. Following mediation analysis with mechanistic factors, is, therefore, of utmost importance.

Limitations

A majority of the hips, for both females (~89%) and males (~73%), reportedly were healthy (KL-0) or early-onset-OA (KL-1). In this study, the cohort was intended to be a mixed population for an initial observation of associations. However, achieving a higher ratio balance between age groups, genders, and subjects with early-onset of hip OA (KL-0–1) vs. mild-to-moderate (KL-2–3 hips) would be further interesting to identify heterogeneous effects or associations via a stratified subgroup analysis. Second, we decided to use $T_{1\rho}$ compositional values alone, and not T_2 consciously in spite of having the data available. This was largely due to the high correlations between the two biomarkers ($T_{1\rho}$ and T_2), and also in order to simplify the analysis with non-duplication of compositional interpretations and limiting multiple dependent variables. However, similar analysis implemented on multi-joint T_2 associations might reveal certain observations that are not already noted in the current study, which might reflect collagen or hydration associations, rather than primarily proteoglycan-driven associations. Third, the slice-thickness of MAPSS sequences, although standard in research and clinical utilization, might suffer from partial volume effects thereby affecting the $T_{1\rho}$ subregional values of both hip and knee. Finally, a small number of subjects are investigated in the study. Due to a lack of previous studies on the compositional association of bilateral multi-joints, a direct sample-size estimation was difficult. In this exploratory study, a possibility of over or underfitting the trends of associations exists. However, LME modeling does not conventionally accommodate regularization approaches applied separately to fixed and random-effects, especially for estimating the nature of the relationship between predictors and outcomes. All significant observations and standardized effects reported in this study can be utilized as a validation tool for sample size estimation and further studies are warranted to overcome these limitations.

Conclusion

In this bilateral hip and knee multi-joint study of subjects with none to moderate radiographic hip OA, we observed positive and negative effects of load-bearing hip cartilage $T_{1\rho}$ (posterior-superior acetabular R_2 and anterior femoral R_5 respectively) on ipsilateral knee patellar $T_{1\rho}$ of whole cartilage as well as all the subregions. On the contrary, posterior femoral R_3 hip cartilage $T_{1\rho}$ had positive effects on the contralateral knee patellar $T_{1\rho}$ of whole cartilage and localized only on the deep and superficial medial subregions.

Supplementary Material

Refer to Web version on PubMed Central for supplementary material.

Acknowledgments

This study was supported by the National Institute of Arthritis and Musculoskeletal and Skin Diseases, part of the National Institutes of Health, under Award Numbers NIH NIAMS R01AR069006 and K24 AR072133. The content is solely the responsibility of the authors and does not necessarily represent the official views of the National Institutes of Health.

References

1. Emami A, Namdari H, Parvizpour F, Arabpour Z. Challenges in osteoarthritis treatment. Tissue Cell. 2023;80:101992. [PubMed: 36462384]
2. Hootman JM, Helmick CG, Barbour KE, Theis KA, Boring MA. Updated projected prevalence of self-reported doctor-diagnosed arthritis and arthritis-attributable activity limitation among US adults, 2015–2040: Projected prevalence of arthritis in the US, 2015–2040. Arthritis Rheumatol 2016;68:1582–1587. [PubMed: 27015600]
3. Barbour KE, Boring M, Helmick CG, Murphy LB, Qin J. Prevalence of severe joint pain among adults with doctor-diagnosed arthritis—United States, 2002–2014. MMWR Morb Mortal Wkly Rep 2016;65:1052–1056. [PubMed: 27711038]
4. Yelin E, Weinstein S, King T. The burden of musculoskeletal diseases in the United States. Semin Arthritis Rheum 2016;46:259–260. [PubMed: 27519477]
5. A treatise on rheumatic gout, or chronic rheumatic arthritis of all the joints. Br Foreign Med Chir Rev 1858;22(43):41–46.
6. Prieto-Alhambra D, Judge A, Javaid MK, Cooper C, Diez-Perez A, Arden NK. Incidence and risk factors for clinically diagnosed knee, hip and hand osteoarthritis: Influences of age, gender and osteoarthritis affecting other joints. Ann Rheum Dis 2014;73:1659–1664. [PubMed: 23744977]
7. Dieppe P, Cushnaghan J, Tucker M, Browning S, Shepstone L. The Bristol “OA500 study”: Progression and impact of the disease after 8 years. Osteoarthr Cartil 2000;8:63–68.
8. Joseph GB, Hilton JF, Jungmann PM, et al. Do persons with asymmetric hip pain or radiographic hip OA have worse pain and structure outcomes in the knee opposite the more affected hip? Data from the Osteoarthritis Initiative. Osteoarthritis Cartilage 2016;24:427–435. [PubMed: 26497607]
9. Block JA, Shakoor N. Lower limb osteoarthritis: Biomechanical alterations and implications for therapy. Curr Opin Rheumatol 2010;22: 544–550. [PubMed: 20592605]
10. Hermann W, Lambova S, Muller-Ladner U. Current treatment options for osteoarthritis. Curr Rheumatol Rev 2018;14:108–116. [PubMed: 28875826]
11. Wang W, Niu Y, Jia Q. Physical therapy as a promising treatment for osteoarthritis: A narrative review. Front Physiol 2022;13:1011407. [PubMed: 36311234]
12. da Costa BR, Reichenbach S, Keller N, et al. Effectiveness of non-steroidal anti-inflammatory drugs for the treatment of pain in knee and hip osteoarthritis: A network meta-analysis. Lancet Lond Engl 2017;390:e21–e33.
13. Shentu C-Y, Yan G, Xu D-C, Chen Y, Peng L-H. Emerging pharmaceutical therapeutics and delivery technologies for osteoarthritis therapy. Front Pharmacol 2022;13:945876. [PubMed: 36467045]
14. Meira EP, Brumitt J. Influence of the hip on patients with patellofemoral pain syndrome: A systematic review. Sports Health 2011;3:455–465. [PubMed: 23016043]
15. van Drongelen S, Braun S, Stief F, Meurer A. Comparison of gait symmetry and joint moments in unilateral and bilateral hip osteoarthritis patients and healthy controls. Front Bioeng Biotechnol 2021;9:756460. [PubMed: 34805115]
16. Eijkenboom JFA, Waarsing JH, Oei EHG, Bierma-Zeinstra SMA, van Middelkoop M. Is patellofemoral pain a precursor to osteoarthritis?: Patellofemoral osteoarthritis and patellofemoral pain patients share aberrant patellar shape compared with healthy controls. Bone Jt Res 2018;7:541–547.
17. Teng HL, MacLeod TD, Link TM, Majumdar S, Souza RB. Higher knee flexion moment during the second half of the stance phase of gait is associated with the progression of osteoarthritis of

the patellofemoral joint on magnetic resonance imaging. J Orthop Sports Phys Ther 2015; 45:656–664. [PubMed: 26161626]

18. Tanamas SK, Teichtahl AJ, Wluka AE, et al. The associations between indices of patellofemoral geometry and knee pain and patella cartilage volume: A cross-sectional study. BMC Musculoskelet Disord 2010; 11:87. [PubMed: 20459700]
19. Samaan MA, Pedoia V, Tanaka MS, Souza RB, Ma CB, Li X. Hip–knee joint coordination patterns are associated with patellofemoral joint cartilage composition in patients with anterior cruciate ligament reconstruction. J Appl Biomech 2022;38:20–28. [PubMed: 35042183]
20. Gallo MC, Wyatt C, Pedoia V, et al. T1ρ and T2 relaxation times are associated with progression of hip osteoarthritis. Osteoarthr Cartil 2016;24:1399–1407.
21. Runhaar J, van Middelkoop M, Oei EHG, Bierma-Zeinstra SMA. Potential surrogate outcomes in individuals at high risk for incident knee osteoarthritis. Osteoarthr Cartil 2023;31:414–420.
22. Stahl R, Luke A, Li X, et al. T1rho, T2 and focal knee cartilage abnormalities in physically active and sedentary healthy subjects versus early OA patients – a 3.0-tesla MRI study. Eur Radiol 2009;19:132–143. [PubMed: 18709373]
23. Yoon MA, Hong S-J, Im AL, Kang CH, Kim BH, Kim IS. Comparison of T1rho and T2 mapping of knee articular cartilage in an asymptomatic population. Korean J Radiol 2016;17:912–918. [PubMed: 27833407]
24. Roach KE, Souza RB, Majumdar S, Pedoia V. Local patterns in 2-year $T_{1\rho}$ and T_2 changes of hip cartilage are related to sex and functional data: A prospective evaluation on hip osteoarthritis participants. J Magn Reson Imaging 2023;57:1042–1053. [PubMed: 35852477]
25. Kellgren JH, Lawrence JS. Radiological assessment of osteo-arthrosis. Ann Rheum Dis 1957;16:494–502. [PubMed: 13498604]
26. Geifman N, Cohen R, Rubin E. Redefining meaningful age groups in the context of disease. Age 2013;35:2357–2366. [PubMed: 23354682]
27. Roach KE, Han M, Link TM, Souza RB, Pedoia V, Majumdar S. Feasibility of simultaneous bilateral hip quantitative MRI. Proc Int Soc Magn Reson Imaging Med 2022. Volume 2022*(30)*. London, UK: International Society of Magnetic Resonance Imaging in Medicine; 2022. p 2309.
28. Pedoia V, Haefeli J, Morioka K, et al. MRI and biomechanics multi-dimensional data analysis reveals R2-R1ρ as an early predictor of cartilage lesion progression in knee osteoarthritis. J Magn Reson Imaging 2018;47:78–90. [PubMed: 28471543]
29. Subburaj K, Valentinitsch A, Dillon AB, et al. Regional variations in MR relaxation of hip joint cartilage in subjects with and without femoralacetabular impingement. Magn Reson Imaging 2013;31:1129–1136. [PubMed: 23684960]
30. Astuto B, Flament I, Namiri NK, et al. Automatic deep learning–assisted detection and grading of abnormalities in knee MRI studies. Radiol Artif Intell 2021;3:e200165. [PubMed: 34142088]
31. Tibrewala R, Pedoia V, Bucknor M, Majumdar S. Principal component analysis of simultaneous PET-MRI reveals patterns of bone–cartilage interactions in osteoarthritis. J Magn Reson Imaging 2020;52:1462–1474. [PubMed: 32207870]
32. Morales AG, Lee JJ, Caliva F, et al. Uncovering associations between data-driven learned qMRI biomarkers and chronic pain. Sci Rep 2021; 11:21989. [PubMed: 34753963]
33. Guo J-B, Liang T, Che Y-J, Yang H-L, Luo Z-P. Structure and mechanical properties of high-weight-bearing and low-weight-bearing areas of hip cartilage at the micro- and nano-levels. BMC Musculoskelet Disord 2020;21:425. [PubMed: 32616028]
34. Li J, Wang Q, Jin Z, Williams S, Fisher J, Wilcox RK. Experimental validation of a new biphasic model of the contact mechanics of the porcine hip. Proc Inst Mech Eng H 2014;228:547–555. [PubMed: 24878736]
35. Jones CE, Mulpuri K, Teo T, Wilson DR, d'Entremont AG. T1ρ and T2 MRI show hip cartilage damage in adolescents with healed Legg-Calvé-Perthes disease. J Pediatr Orthop B 2022;31:344–349. [PubMed: 34139748]
36. Watanabe A, Boesch C, Siebenrock K, Obata T, Anderson SE. T2 mapping of hip articular cartilage in healthy volunteers at 3T: A study of topographic variation. J Magn Reson Imaging 2007;26:165–171. [PubMed: 17659572]

37. Häuselmann HJ, Flechtenmacher J, Michal L, et al. The superficial layer of human articular cartilage is more susceptible to interleukin-1–induced damage than the deeper layers. Arthritis Rheum 1996;39:478–488. [PubMed: 8607897]

38. Eijkenboom JFA, van der Heijden RA, de Kanter JLM, Oei EH, Bierma-Zeinstra SMA, van Middelkoop M. Patellofemoral alignment and geometry and early signs of osteoarthritis are associated in patellofemoral pain population. Scand J Med Sci Sports 2020;30:885–893. [PubMed: 32096249]

39. Anderson AS, Loeser RF. Why is osteoarthritis an age-related disease? Best Pract Res Clin Rheumatol 2010;24:15–26. [PubMed: 20129196]

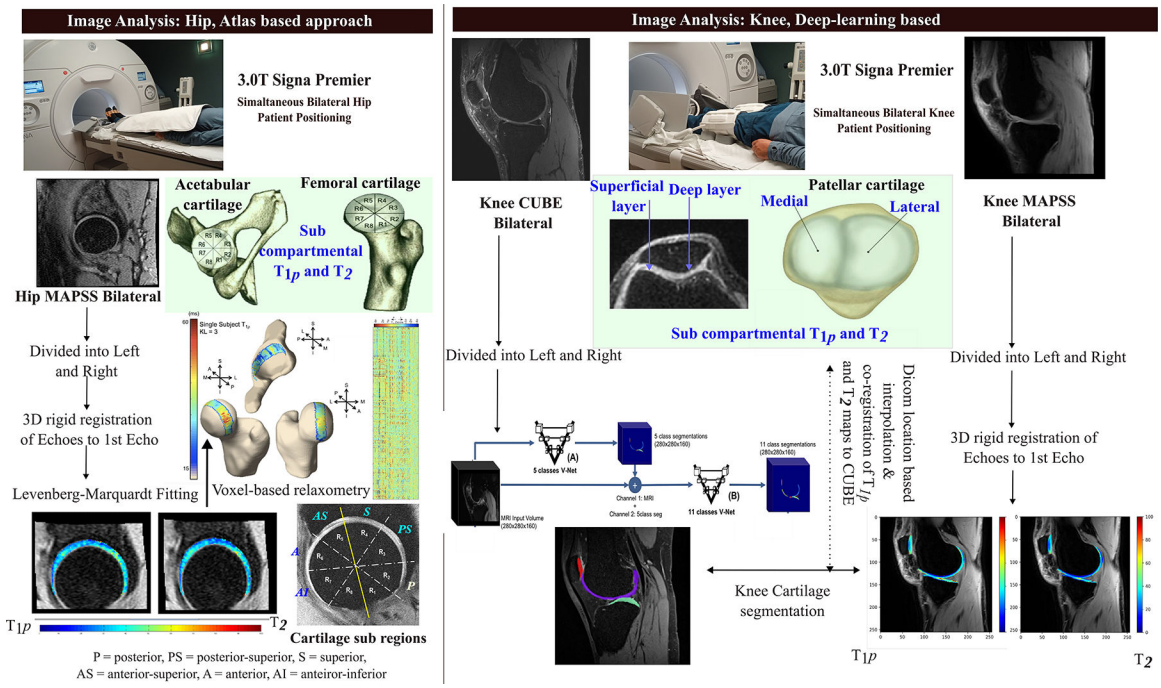

FIGURE 1:

Schema of methodology: Image acquisition, processing, segmentation, analysis, and evaluation.

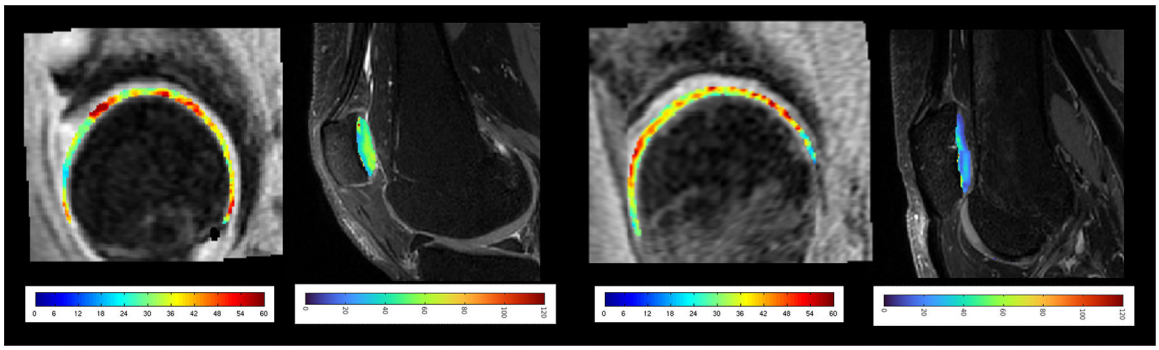

Patient 1: Age =58, Female, Right Hip, KL = 3, Right Knee, KL = 0

(A1) **(A2)**

Patient 2: Age =49, Female, Right Hip, KL = 0, Right Knee, KL = 0

(B1) **(B2)**

Case 1: Intra-limb analysis

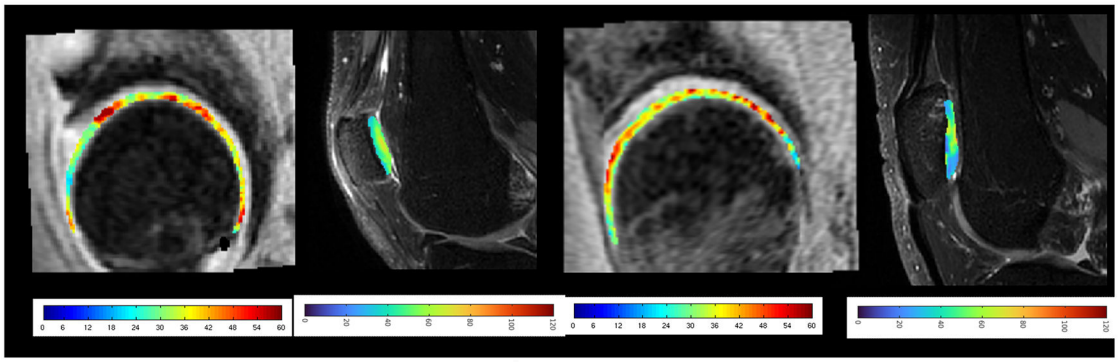

Patient 1: Age =58, Female, Right Hip, KL = 3, Left Knee, KL = 0

(C1) **(C2)**

Patient 2: Age =49, Female, Right Hip, KL = 0, Left Knee, KL = 0

(D1) **(D2)**

Case 2: Inter-limb analysis

FIGURE 2:

Intra-limb: (a1, a2) Demonstrative examples case of a female Hip-OA subject, right femoral whole cartilage $T_{1\rho}$ (KL = 3) vs. ipsilateral patellar $T_{1\rho}$ (KL = 0). (b1, b2) Demonstrative examples case of a female healthy subject, right femoral whole cartilage $T_{1\rho}$ (KL = 0) vs. ipsilateral patellar $T_{1\rho}$ (KL = 0). Inter-limb: (c1, c2) Demonstrative examples case of a female Hip-OA subject, right femoral whole cartilage $T_{1\rho}$ (KL = 3) vs. contralateral patellar $T_{1\rho}$ (KL = 0). (d1, d2) Demonstrative examples case of a female healthy subject, right femoral whole cartilage $T_{1\rho}$ (KL = 0) vs. contralateral patellar $T_{1\rho}$ (KL = 0). KL indicates Kellgren–Lawrence.

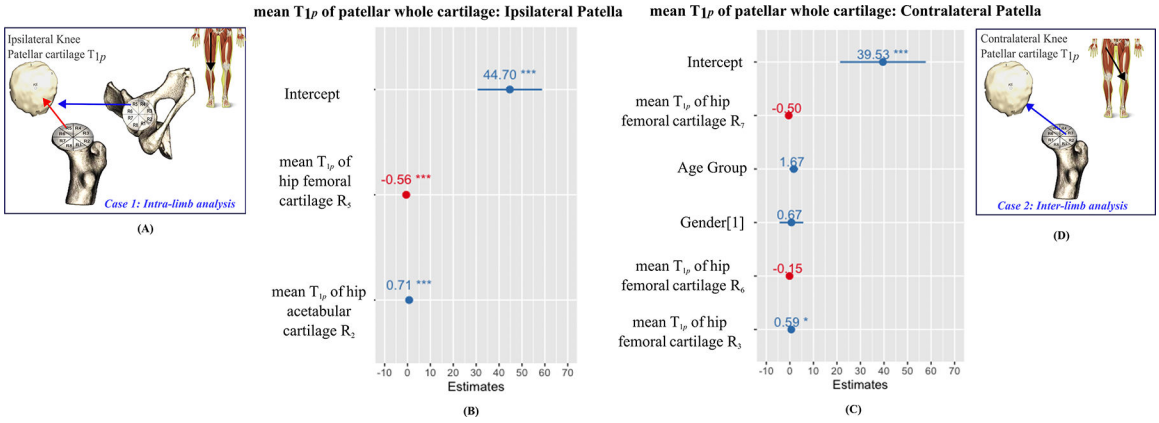

FIGURE 3:

Analysis results summarized for Intra-limb: (a) Pictorial representation of the significant positive and negative fixed-effects on the primary outcome, ipsilateral knee patellar $T_{1\rho}$ (positive indicated in blue, negative in red). (b) Fixed-effects and their estimates plotted, for the best predictor mixed-effects model, Model-3: Primary outcome ~ mean $T_{1\rho}$ of hip femoral R_5 cartilage + mean $T_{1\rho}$ of hip acetabular R_2 cartilage) + (1 | Participant-ID). Analysis results summarized for Inter-limb: (c) Fixed-effects and their estimates plotted, for the best predictor mixed-effects model, Model-6: Primary outcome ~ mean $T_{1\rho}$ of hip femoral R_7 cartilage + age-group + gender + mean $T_{1\rho}$ of hip femoral R_6 cartilage + mean $T_{1\rho}$ of hip femoral R_3 cartilage) + (1 | Participant-ID). (d) Pictorial representation of the significant positive and negative fixed-effects on the primary outcome, contralateral knee patellar $T_{1\rho}$ (positive indicated in blue, negative in red).

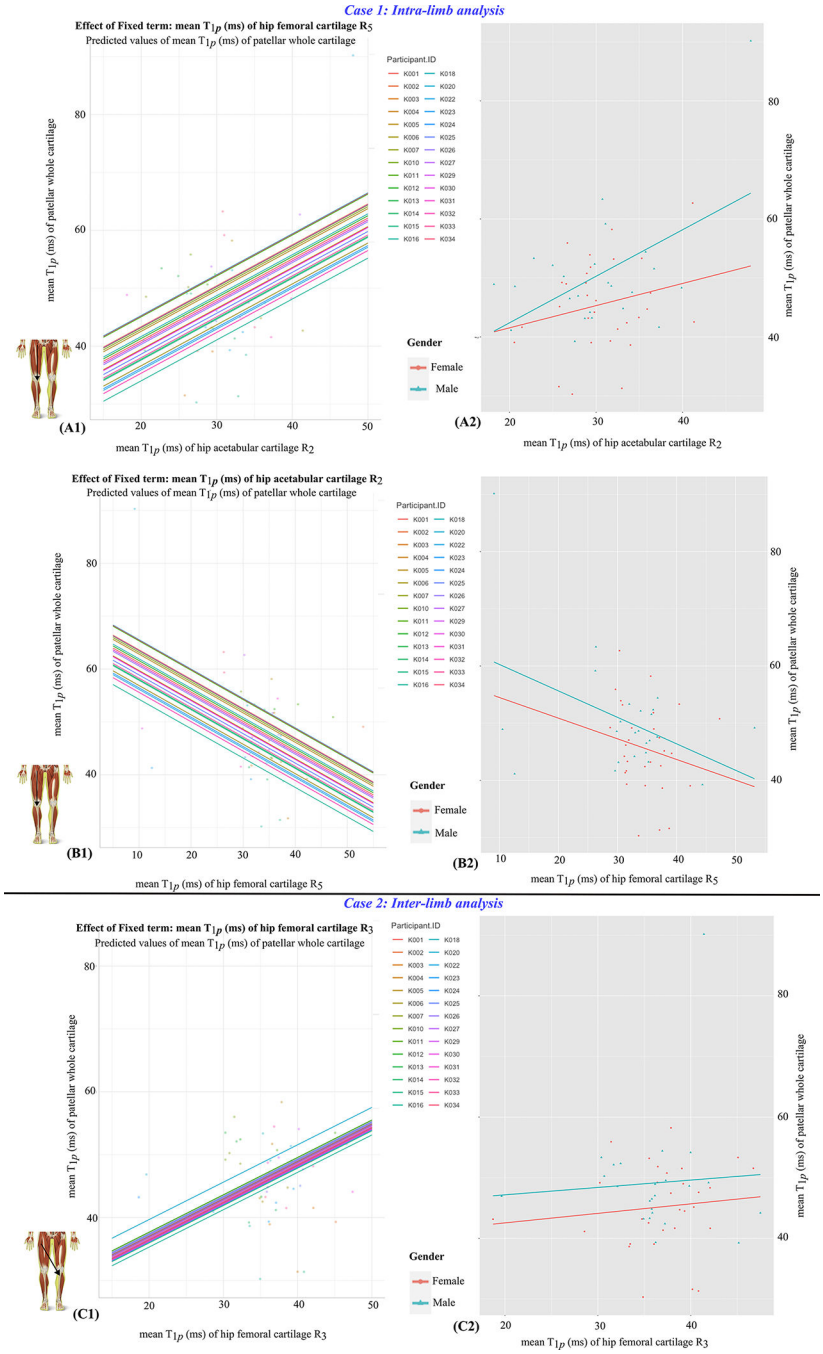

FIGURE 4:

Intra-limb: (a1) Plotted effect of mean $T_{1\rho}$ of hip acetabular R_2 on mean $T_{1\rho}$ of patellar-whole-cartilage, Model-3. (a2) The scatterplot A1 is stratified for the Gender (Female and Male) of subjects. (b1) Plotted effect of mean $T_{1\rho}$ of hip femoral R_5 on mean $T_{1\rho}$ of patellar-whole-cartilage, Model-3. (b2) The scatterplot B1 is stratified for the Gender (Female and Male) of subjects. Inter-limb: (c1) Plotted effect of mean $T_{1\rho}$ of hip femoral R_3 on mean

$T_{1\rho}$ of patellar-whole-cartilage, Model-6. (c2) The scatterplot C1 is stratified for the Gender (Female and Male) of subjects.

TABLE 1.

Acquisition Parameters for MRI Sequences Utilized in This Study

Morphological Bilateral MRI Sequences									
Sequence	**Image Contrast**	**TR (msec)**	**TE (msec)**	**FOV (cm × cm)**	**Resolution (mm^2)**	**Acquisition Matrix**	**Reconstruction Matrix**	**Slice Thickness (mm)/Number of Slices (Approx.)**	**Scan Time**
Hip CUBE Coronal	3D PD fat saturated	1200	20.62	16 × 32 (S/I × R/L)	0.8 × 0.8	200 × 400	512 × 1024	0.8/210–230	12 minutes 30 seconds
Knee CUBE Sagittal	3D PD fat saturated	1202	26.62	15 × 15	0.6 × 0.6	256 × 256	512 × 512	0.6/540–550	12 minutes
Compositional (Combined $T_{1\rho}$ and T_2) Bilateral MRI Sequences									
Sequence	**TSL (msec)**	**TE (msec)**	**Spin Lock Frequency**	**FOV (cm × cm)**	**Resolution (mm^2)**	**Acquisition Matrix**	**Reconstruction Matrix**	**Slice Thickness (mm)/Number of Slices (Approx.)**	**Scan Time**
Hip MAPSS Sagittal	0, 15, 30, 45	0, 10.4, 20.8, 41.6	300 Hz	14 × 14	0.55 × 1.09	256 × 128	256 × 256	4/70–80	16 minutes 30 seconds
Knee MAPSS Sagittal	0, 10, 40, 80	0, 12.8, 25.7, 51.4	500 Hz	14 × 14	0.55 × 1.09	256 × 128	256 × 256	4/80–90	10 minutes 30 seconds

TSL = time of spin lock; TE = echo time; TR = repetition time; FOV = field of view; MAPSS = magnetization-prepared angle-modulated partitioned k-space spoiled gradient-echo snapshots.

TABLE 2.

Demographic, Clinical, Functional, and Compositional Description of the Study Cohort

Descriptor	Gender Identified as Women (N = 15, 30 Hips, and 30 Knees)	Gender Identified as Men (N = 13, 26 Hips, and 26 Knees)
Age (years)	54.2 ± 11.71	58.6 ± 13.45
BMI	22.9 ± 2.63	26.02 ± 4.55
Hip KL 0[a] (no OA)	10 (33.3%)	7 (26.92%)
Hip KL 1[a] (minimal/doubtful)	17 (56.35%)	12 (46.15%)
Hip KL 2[a] (mild)	2 (6.66%)	5 (19.23%)
Hip KL 3[a] (moderate)	1 (3.33%)	2 (7.69%)
Knee KL 0[a] (no OA)	20 (66.66%)	17 (50%)
Knee KL 1[a] (minimal/doubtful)	10 (33.33%)	9 (36.67%)
Knee KL 2[a] (mild)	0 (0%)	0 (0%)
Knee KL 3[a] (moderate)	0 (0%)	0 (0%)
Mean $T_{1\rho}$ values: Femoral R_2 (msec)	36.57 ± 5.90	33.46 ± 6.35
Mean $T_{1\rho}$ values: Femoral R_3 (msec)	36.94 ± 5.27	35.59 ± 6.72
Mean $T_{1\rho}$ values: Femoral R_4 (msec)	33.03 ± 6.02	31.38 ± 5.66
Mean $T_{1\rho}$ values: Femoral R_5 (msec)	34.62 ± 5.81	32.89 ± 8.31
Mean $T_{1\rho}$ values: Femoral R_6 (msec)	32.28 ± 4.92	30.09 ± 6.17
Mean $T_{1\rho}$ values: Femoral R_7 (msec)	32.16 ± 5.27	26.98 ± 5.26
Mean $T_{1\rho}$ values: Acetabular R_2 (msec)	30.42 ± 5.33	31.11 ± 7.21
Mean $T_{1\rho}$ values: Acetabular R_3 (msec)	33.53 ± 5.46	35.89 ± 5.20
Mean $T_{1\rho}$ values: Acetabular R_4 (msec)	30.28 ± 3.54	32.31 ± 6.61
Mean $T_{1\rho}$ values: Acetabular R_5 (msec)	30.95 ± 4.76	32.00 ± 7.42
Mean $T_{1\rho}$ values: Acetabular R_6 (msec)	31.42 ± 7.08	29.95 ± 8.84
Mean $T_{1\rho}$ values: Patellar-whole-cartilage (msec)	45.20 ± 7.01	49.12 ± 9.72
Mean $T_{1\rho}$ values: Patellar DM cartilage (msec)	45.72 ± 7.87	51.72 ± 14.09
Mean $T_{1\rho}$ values: Patellar DL cartilage (msec)	43.46 ± 7.9	48.98 ± 13.52

J Magn Reson Imaging. Author manuscript; available in PMC 2024 July 28.

Descriptor	Gender Identified as Women (N = 15, 30 Hips, and 30 Knees)	Gender Identified as Men (N = 13, 26 Hips, and 26 Knees)
Mean $T_{1\rho}$ values: Patellar SM cartilage (msec)	46.05 ± 8.79	51.21 ± 14.03
Mean $T_{1\rho}$ values: Patellar SL cartilage (msec)	45.84 ± 10.58	50.09 ± 12.34

Information presented as mean ± SD, unless noted otherwise. KL = Kellgren-Lawrence score; AODL = activities of daily life; QOL = quality of life; DM = deep medial; DL = deep lateral; SM = superficial medial; SL = superficial lateral.

[a]Data expressed as counts (percentage of the total sample).

TABLE 3.

Case 1, Intra-Limb Analysis: Stepwise Linear Mixed-Effects Modeling (LME) Between Hip Cartilage Subregional Mean $T_{1\rho}$ vs. Ipsilateral Limb Knee Patellar (Whole Cartilage) Mean $T_{1\rho}$

Knee Patellar $T_{1\rho}$ Values (Mean of Whole Cartilage)						
	LME Model 1	**LME Model 2**	**LME Model 3**	**LME Model 4**	**LME Model 5**	**LME Model 6**
***P*-value (ANOVA)**	**NA**	**0.0018362****	**0.0001829*****	**0.9466756**	**0.1589069**	**0.2312886**
Predictors	**Estimates** **CI** **P**	**Estimates** **CI** **P**	**Estimates** **CI** **P**	**Estimates** **CI** **P**	**Estimates** **CI** **P**	**Estimates** **CI** **P**
(Intercept)	47.67 44.96–50.37 **<0.001*****	64.90 54.02–75.79 **<0.001*****	44.70 30.61–58.79 **<0.001*****	44.51 29.57–59.44 **<0.001*****	41.58 26.23–56.94 **<0.001*****	43.15 27.72–58.59 **<0.001*****
Mean $T_{1\rho}$ values of hip femoral R_5 cartilage		−0.52 −0.84 to −0.20 **0.002****	−0.56 − 0.84 to −0.27 **<0.001*****	−0.57 − 1.09 to −0.05 **0.032****	−0.50 − 1.01 to 0.02 0.058	−0.61 − 1.15 to −0.07 **0.027****
Mean $T_{1\rho}$ values of hip acetabular R_2 cartilage			0.71 0.36–1.06 **<0.001*****	0.71 0.35–1.06 **<0.001*****	0.71 0.36–1.06 **<0.001*****	0.77 0.41–1.12 **<0.001*****
Mean $T_{1\rho}$ values of hip femoral R_6 cartilage				0.03 −0.65 to 0.70 0.940	−0.01 −0.68 to 0.65 0.966	0.30 −0.53 to 1.14 0.468
Gender [1 = Male]					3.34 − 1.30 to 7.97 0.155	2.72 −2.00 to 7.44 0.252
Mean $T_{1\rho}$ values of hip femoral R_7 cartilage						−0.30 −0.80 to 0.20

Knee Patellar $T_{1\rho}$ Values (Mean of Whole Cartilage)						
	LME Model 1	**LME Model 2**	**LME Model 3**	**LME Model 4**	**LME Model 5**	**LME Model 6**
***P*-value (ANOVA)**	**NA**	**0.0018362****	**0.0001829*****	**0.9466756**	**0.1589069**	**0.2312886**
Predictors	**Estimates** **CI** **P**	**Estimates** **CI** **P**	**Estimates** **CI** **P**	**Estimates** **CI** **P**	**Estimates** **CI** **P**	**Estimates** **CI** **P**
						0.234
Random-effects						
σ^2	64.43	51.72	35.45	35.20	35.96	34.50
τ_{00}	$17.12_{Participant.ID}$	$17.01_{Participant.ID}$	$19.42_{Participant.ID}$	$19.79_{Participant.ID}$	$16.09_{Participant.ID}$	$16.40_{Participant.ID}$
ICC	0.21	0.25	0.35	0.36	0.31	0.32
N	$28_{Participant.ID}$	$28_{Participant.ID}$	$28_{Participant.ID}$	$28_{Participant.ID}$	$28_{Participant.ID}$	$28_{Participant.ID}$
Observations	56	56	56	56	56	56
Marginal R^2/Conditional R^2	0.000/0.210	0.173/0.378	**0.352/0.581**	0.352/0.585	0.385/0.575	0.404/0.596

Significant predictor-outcome associations are highlighted in bold. CI = confidence interval; ICC = intra-class-coefficient. Statistical significance codes for predictor models:

*"***"*
0.001

*"**"*
0.01

""*
0.05.

The best-performing statistically significant predictor (*Model 3* in this case) associated with the highest marginal R^2, conditional R^2, and ICC values, is highlighted. All the models were estimated using maximum-likelihood and nloptwrap optimizer. Standardized parameters were obtained by fitting the model on a standardized version of the dataset. 95% CIs and *P*-values were computed using a Wald t-distribution approximation.

The fixed-effects formula for the best predictor model (Model 3) was: (Knee patellar $T_{1\rho}$ values [mean of whole cartilage] ~ mean $T_{1\rho}$ values of hip femoral R_5 cartilage + mean $T_{1\rho}$ values of hip acetabular R_2 cartilage), including Participant-ID as a random-effect (formula: ~1 | Participant-ID). The model's total explanatory power is substantial (conditional R^2 = 0.581), and the part related to the fixed-effects alone (marginal R^2) is 0.352. The model's intercept, (corresponding to fixed-effects = 0), is at 44.70 (95% CI [30.61 to 58.79], t(49) = 6.37, $P < 0.001$). Within Model 3: the effect of mean $T_{1\rho}$ values of hip femoral R_5 cartilage is statistically significant and negative, and the effect of mean $T_{1\rho}$ values of hip acetabular R_2 cartilage is statistically significant and positive.

TABLE 4.

Case 1, Intra-Limb Analysis: The Best Predictor Linear Mixed-Effects (LME) Model (Model 3) Selected From Table 3, Is Evaluated for Finding Associations Between Hip Cartilage Subregional Mean $T_{1\rho}$ vs. Secondary Outcome, Ipsilateral Limb Knee Patellar (Subregional Cartilages, Deep-Medial/DM, Superficial-Medial/SM, Superficial-Lateral/SL, Deep-Lateral/DL) Mean $T_{1\rho}$

Knee Patellar $T_{1\rho}$ Values				
	Deep Medial Cartilage	**Superficial Medial Cartilage**	**Superficial Lateral Cartilage**	**Deep Lateral Cartilage**
	Estimates	**Estimates**	**Estimates**	**Estimates**
	CI	**CI**	**CI**	**CI**
Predictors	**P**	**P**	**P**	**P**
(Intercept)	43.83	41.42	47.35	50.46
	24.49–63.18	19.97–62.87	27.40–67.30	31.84–69.08
	<0.001 ***	**<0.001** ***	**<0.001** ***	**<0.001** ***
Mean $T_{1\rho}$ values of hip femoral R_5 cartilage	−0.55	−0.59	−0.55	−0.64
	−0.94 to −0.16	−1.02 to −0.16	−0.95 to −0.15	−1.01 to −0.26
	0.006 **	**0.009** **	**0.008** **	**0.001** **
Mean $T_{1\rho}$ values of hip acetabular R_2 cartilage	0.77	0.91	0.63	0.56
	0.27–1.27	0.37–1.46	0.11–1.15	0.08–1.04
	0.003 **	**0.001** ***	**0.018** *	**0.024** *
Random-effects				
σ^2	98.95	101.01	111.60	97.21
τ_{00}	$4.73_{\text{Participant.ID}}$	$24.05_{\text{Participant.ID}}$	$0.00_{\text{Participant.ID}}$	$0.00_{\text{Participant.ID}}$
ICC	0.05	0.19		
N	$28_{\text{Participant.ID}}$	$28_{\text{Participant.ID}}$	$28_{\text{Participant.ID}}$	$28_{\text{Participant.ID}}$
Observations	56	56	56	56
Marginal R^2/Conditional R^2	0.238/0.273	0.250/0.394	0.191/NA	0.232/NA

CI = confidence interval; ICC = intra-class-coefficient. The ICC and conditional R^2 are termed NA, in case, the variances within the random-effect (Participant-ID) were found ignorable. All the models were estimated using maximum-likelihood and nloptwrap optimizer. Standardized parameters were obtained by fitting the model on a standardized version of the dataset. 95% CIs and *P*-values were computed using a Wald t-distribution approximation. Statistical significance codes for predictor models:

*"***"*
0.001

*"**"*
0.01

""*
0.05.

The fixed-effects formula for the model was: (Knee patellar $T1\rho$ values [mean of DM/SM/SL/DL] ~ mean $T1\rho$ values of hip femoral R_5 cartilage + mean $T1\rho$ values of hip acetabular R_2 cartilage), including Participant-ID as a random-effect (formula: ~1 | Participant-ID). The model's total explanatory powers for DM, SM, SL, and DL are moderate to substantial. The statistically significant (*P*-value ≤ 0.05) fixed-effects for each model (DM/SM/SL/DL) are highlighted in bold (if present).

TABLE 5.

Case 2, Inter-Limb Analysis: linear Mixed-Effects (LME) Modeling Between Hip Cartilage Subregional Mean $T_{1\rho}$ vs. Contralateral Limb Knee Patellar (Whole Cartilage) Mean $T_{1\rho}$

Knee Patellar $T_{1\rho}$ Values (Mean of Whole Cartilage)						
	LME Model 1	**LME Model 2**	**LME Model 3**	**LME Model 4**	**LME Model 5**	**LME Model 6**
***P*-value (ANOVA)**	**NA 1**	**0.04110***	**0.33954**	**0.22076**	**0.36821**	**0.04846****
Predictors	**Estimates** **CI** **P**	**Estimates** **CI** **P**	**Estimates** **CI** **P**	**Estimates** **CI** **P**	**Estimates** **CI** **P**	**Estimates** **CI** **P**
(Intercept)	46.95 44.55–49.34 **<0.001*****	59.24 47.54–70.93 **<0.001*****	55.63 41.79–69.47 **<0.001*****	53.29 39.10–67.47 **<0.001*****	49.91 34.02–65.80 **<0.001*****	39.53 21.32–57.74 **<0.001*****
Mean $T_{1\rho}$ values of hip femoral R_7 cartilage		−0.41 −0.79 to −0.03 **0.036****	−0.32 − 0.74 to 0.10 0.128	−0.34 −0.76 to 0.07 0.105	−0.52 −1.08 to 0.05 0.073	−0.50 −1.05 to 0.05 0.074
Age-group			2.32 − 2.54 to 7.19 0.342	1.59 −3.35 to 6.54 0.520	1.05 − 4.02 to 6.13 0.678	0.67 −4.38 to 5.72 0.791
Gender [1 = Male]				1.07 −0.67 to 2.81 0.224	1.28 − 0.52 to 3.08 0.159	1.67 −0.15 to 3.49 0.072
Mean $T_{1\rho}$ values of hip femoral R_6 cartilage					0.26 −0.31 to 0.83 0.364	−0.15 −0.85 to 0.55 0.675
Mean $T_{1\rho}$ values of hip femoral R_3 cartilage						0.59 0.01–1.18

Knee Patellar $T_{1\rho}$ Values (Mean of Whole Cartilage)						
	LME Model 1	**LME Model 2**	**LME Model 3**	**LME Model 4**	**LME Model 5**	**LME Model 6**
***P*-value (ANOVA)**	**NA 1**	**0.04110***	**0.33954**	**0.22076**	**0.36821**	**0.04846****
Predictors	**Estimates** **CI** **P**	**Estimates** **CI** **P**	**Estimates** **CI** **P**	**Estimates** **CI** **P**	**Estimates** **CI** **P**	**Estimates** **CI** **P**
Random-effects						**0.047****
σ^2	63.74	65.00	63.91	62.16	60.56	52.73
τ_{00}	$6.80_{Participant.ID}$	$0.00_{Participant.ID}$	$0.00_{Participant.ID}$	$0.00_{Participant.ID}$	$0.68_{Participant.ID}$	$4.41_{Participant.ID}$
ICC	0.10				0.01	0.08
N	$28_{Participant.ID}$	$28_{Participant.ID}$	$28_{Participant.ID}$	$28_{Participant.ID}$	$28_{Participant.ID}$	$28_{Participant.ID}$
Observations	56	56	56	56	56	56
Marginal R^2/ Conditional R^2	0.000/0.096	0.080/NA	0.096/NA	0.121/NA	0.134/0.144	0.195/0.257

Significant predictor-outcome associations are highlighted in bold. CI = confidence interval; AIC = Akaike-information-criterion; Est = estimates; ICC = intra-class-coefficient. Statistical significance codes for predictor models:

*"***"* 0.001

*"**"* 0.01

""* 0.05.

The best-performing statistically significant predictor model (*Model 6*, in this case) associated with the highest marginal R^2, conditional R^2, and ICC values, is highlighted. All the models were estimated using maximum-likelihood and nloptwrap optimizer. Standardized parameters were obtained by fitting the model on a standardized version of the dataset. 95% CIs and *P*-values were computed using a Wald t-distribution approximation.

The fixed-effects formula for the best predictor model (Model 5) was: (Knee patellar $T_{1\rho}$ values (mean of whole cartilage) ~ mean $T_{1\rho}$ values of hip femoral R7 cartilage + age-group + gender + mean $T_{1\rho}$ values of hip femoral R cartilage + mean $T_{1\rho}$ values of hip femoral R3 cartilage), including Participant-ID as a random-effect (formula: ~1 | Participant-ID). The model's total explanatory power is moderate (conditional R^2 = 0.258), and the part related to the fixed-effects alone (marginal R^2) is 0.195. The model's intercept, (corresponding to fixed-effects = 0), is at 39.53 (95% CI [21.32 to 57.74], t(46) = 4.37, $P < .001$). Within Model 6: the effect of mean $T_{1\rho}$ values of hip femoral R3 cartilage, is statistically significant and positive. The effects of other variables in this model, however additive, are statistically non-significant.

TABLE 6.

Case 2, Inter-Limb Analysis: The Best Predictor Multivariate Mixed-Effects Model (Model 5) Selected From Table 4, Is Evaluated for Finding Associations Between Hip-Cartilage Subregional Mean $T_{1\rho}$ vs. Secondary Outcome, Contralateral Limb Knee Patellar (Subregional Cartilages, DM, SM, SL, DL) Mean $T_{1\rho}$

Knee Patellar $T_{1\rho}$ Values				
	Deep Medial Cartilage	**Superficial Medial Cartilage**	**Superficial Lateral Cartilage**	**Deep Lateral Cartilage**
	Estimates	**Estimates**	**Estimates**	**Estimates**
	CI	**CI**	**CI**	**CI**
Predictors	***P***	***P***	***P***	***P***
(Intercept)	35.72	40.38	41.31	35.70
	11.40–60.05	16.74–64.02	16.03–66.59	11.19–60.21
	0.005 **	**0.001** ***	**0.002** **	**0.005** **
Mean $T_{1\rho}$ values of hip femoral R_7 cartilage	−0.42	−0.74	−0.51	−0.13
	−1.16 to 0.32	−1.46 to −0.02	−1.28 to 0.26	−0.88 to 0.62
	0.257	**0.044** **	0.189	0.727
Age-group	2.47	2.65	1.56	1.35
	0.07 to 4.87	0.30 to 5.00	−0.94 to 4.05	−1.07 to 3.78
	0.044 **	**0.028** **	0.216	0.266
Gender [1 = Male]	2.66	−0.04	0.93	4.02
	−4.01 to 9.32	−6.55 to 6.47	−6.00 to 7.86	−2.70 to 10.73
	0.427	0.990	0.788	0.235
Mean $T_{1\rho}$ values of hip femoral R_6 cartilage	−0.17	−0.47	−0.25	−0.24
	−1.11 to 0.77	−1.39 to 0.44	−1.23 to 0.73	−1.19 to 0.71
	0.719	0.302	0.609	0.612
Mean $T_{1\rho}$ values of hip femoral R_3 cartilage	0.60	1.01	0.67	0.43
	−0.19 to 1.40	0.25 to 1.78	−0.16 to 1.50	−0.37 to 1.24
	0.133	**0.011** **	0.109	0.281

Knee Patellar $T_{1\rho}$ Values				
	Deep Medial Cartilage	**Superficial Medial Cartilage**	**Superficial Lateral Cartilage**	**Deep Lateral Cartilage**
	Estimates	**Estimates**	**Estimates**	**Estimates**
	CI	**CI**	**CI**	**CI**
Predictors	***P***	***P***	***P***	***P***
Random-effects				
σ^2	105.58	95.22	114.07	107.20
τ_{00}	$0.00_{Participant.ID}$	$3.02_{Participant.ID}$	$0.00_{Participant.ID}$	$0.00_{Participant.ID}$
ICC		0.03		
N	$28_{Participant.ID}$	$28_{Participant.ID}$	$28_{Participant.ID}$	$28_{Participant.ID}$
Observations	56	56	56	56
Marginal R^2/Conditional R^2	0.170/NA	0.259/0.282	0.122/NA	0.100/NA

CI = confidence interval; ICC = intra-class-coefficient. The ICC and conditional R^2 are termed NA, in case, the variances within the random-effect (Participant-ID) were found ignorable. All the models were estimated using maximum-likelihood and nloptwrap optimizer. Standardized parameters were obtained by fitting the model on a standardized version of the dataset. 95% CIs and *P*-values were computed using a Wald t-distribution approximation. Statistical significance codes for predictor models:

*"***"*
0.001

*"**"*
0.01

""*
0.05.

The fixed-effects formula for the model was: (Knee patellar $T_{1\rho}$ values (mean of DM/SM/SL/DL) ~ mean $T_{1\rho}$ values of hip femoral R7 cartilage + age-group + gender + mean Tip values of hip femoral R6 cartilage + mean $T_{1\rho}$ values of hip femoral R3 cartilage), including Participant-ID as a random-effect (formula: ~1 | Participant-ID). The model's total explanatory powers for DM, SM, SL, and DL are moderate. The statistically significant (*P*-value ≤ 0.05) fixed-effects for each model (DM/SM/SL/DL) are highlighted in bold (if present).